Spatiotemporal dynamics of succession and growth limitation of phytoplankton for nutrients and light in a large shallow lake

Xuemei Liu [a,b], Liwen Chen [a], Guangxin Zhang [a,*], Jingjie Zhang [a,c,d,*], Yao Wu [a], Hanyu Ju [a,b]

[a] Northeast Institute of Geography and Agroecology, Chinese Academy of Sciences. Changchun 130102, China
[b] University of the Chinese Academy of Sciences, Beijing 100049, China
[c] Environmental Research Institute, National University of Singapore, Kent Ridge 117576, Singapore
[d] Shenzhen Municipal Engineering Lab of Environmental IoT Technologies, Southern University of Science and Technology, Shenzhen, 518055, China

ARTICLE INFO

ABSTRACT

Understanding the limiting factors of phytoplankton growth and competition is crucial for the restoration of aquatic ecosystems. However, the role and synergistic effect of co-varying environmental conditions, such as nutrients and light on the succession of phytoplankton community remains unclear. In this study, a hydrodynamic-ecological modeling approach was developed to explore phytoplankton growth and succession under co-varying environmental conditions (nutrients, total suspended solids (TSS) and variable N:P ratios) in a large shallow lake called Lake Chagan, in Northeast China. A phytoplankton bloom model was nested in the ecological modeling approach. In contrast to the traditonal ecological modeling, competition between phytoplankton species in our study was modeled at both the species/functional group and phenotype levels. Six phytoplankton functional groups, namely diatoms, green algae, *Anabaena, Microcystis, Aphanizomenon* and *Oscillatoria* and each of them with three limitation types (i.e., light-limitation, nitrogen-limitation and phosphorus-limitation) were included in the bloom model. Our results demonstrated that the average biomass proportion of the three limitation types (light-limitation, nitrogen-limitation and phosphorus-limitation) in the six phytoplankton function groups accounted for approximately 50%, 37% and 23% of the total phytoplankton biomass, respectively. TSS suppressed the growth of diatoms and green algae, but favored the dominance of cyanobacteria in Lake Chagan, especially in the turbid water phase (TSS $\geq$ 60 mg/L). In addition, it was reported that the potential of either N-fixing or non-N-fixing cyanobacterial blooming along the gradients of N:P ratios could exist under the influence of the co-environmental factors in the lake. The proportion of non-N-fixing cyanobacteria (i.e., *Microcystis* and *Oscillatoria*) exceeded the proportion of N-fixing cyanobacteria (i.e., *Anabaena* and *Aphanizomenon*) when the N:P ratios exceeded 20. Non-N-fixing cyanobacteria would become dominant at higher TSS concentrations and lower light intensities in the turbid water. N-fixing cyanobacteria favored lower N:P ratios and higher light intensities in the clearwater phase (where TSS $\leq$ 60 mg/L). To sustain a good ecological status in the lake, our results suggest that nutrient and TSS levels in the lake should be maintained at or below the thresholds (TN $\leq$ 1.5 mg/L; TP $\leq$ 0.1 mg/L; N:P ratios between 15 and 20; and TSS $\leq$ 60 mg/L). These findings can help improve water quality management practices to restore aquatic ecosystems.

© 2021 Elsevier Ltd. All rights reserved.

1. Introduction

Phytoplankton is a prominent indicator of lake ecosystem health and the over-proliferation of phytoplankton is one of the most challenging environmental problems (Huisman et al., 2018). Climate change (such as rising temperature, change in rainfall pattern and drought conditions) and anthropogenic activities (such urbanization and modern agricultural practices) are the main drivers of the over-proliferation of phytoplankton and species succession, which threaten water security and sustainable development of fisheries (Axler et al., 1981; Markensten and Pierson, 2007; Newcombe et al., 2012; Reichwaldt and Ghadouani, 2012; Sakamoto et al., 2020). Harmful algal blooms (HABs) refer mainly to the over-proliferation of algae in marine and freshwater environments (e.g., cyanobacteria, dinoflagellates and diatoms). Toxic and off-flavor compounds not only have an adverse impact on human health, but also threaten the sustainable development of aquatic ecosystems and local economies (Ross et al., 2006; Paerl and Huisman, 2008; Preece et al., 2017; Huisman et al., 2018). However,

---

* Corresponding authors.
  E-mail addresses: zhgx@iga.ac.cn (G. Zhang), lakejz@gmail.com (J. Zhang).

quantifying the relationship between the nutrients and the proliferation of specific algal species and identifying the main driving forcing and the mechanism behind the blooms are very complex and challenging (Glibert and Burkholder, 2011). Therefore, an effective control of HABs is important for lake water quality management under the increase of anthropogenic activities and climate pressure on aquatic ecosystems worldwide.

The phytoplankton community structure and primary production are important ecosystem indicators for evaluating lake ecosystem health (Boyer et al., 2009), which are affected by various abiotic factors such as nutrients (N, P), physical light, temperature, wind speed, precipitation, and pH (McCarthy and Goldman, 1979; Sunda et al., 1997; Jakobsen et al., 2015; Stockwell et al., 2020), and biotic factors such as planktonic herbivores (Paerl et al., 2001; Smayda, 2008). Extensive studies have suggested that both absolute levels and ratios of nutrients (nitrogen to phosphorus) and light are the main driving factors affecting phytoplankton growth and succession (Smith et al., 1999; Abell et al., 2010; Assemany et al., 2015; Søndergaard et al., 2017). Nutrient loading associated with agricultural land use, such as the irrigation discharge, would lead to a shift in N:P ratios and higher nutrient concentrations, resulting in species succession and higher biomass in the receiving water bodies (Lie et al., 2011; Paerl et al., 2011; Paerl et al., 2019; Diatta et al., 2020). Nutrient uptake by phytoplankton at an optimum ratio of 16:1 may promote phytoplankton growth, but proliferation of each phytoplankton species may occur differently, especially, under the conditions of nutrient imbalance (Redfield, 1958; Teubner and Dokulil, 2002; Faithfull et al., 2011; Glibert et al., 2011; Reeder, 2017). The competition of phytoplankton for nutrients and light has resulted in considerable studies related to lake ecosystems (Zeng et al., 2015; Dai et al., 2020). Phytoplankton production can be impaired by both nutrients and light. In addition, there exists a co-limitation of phytoplankton growth by nutrients and light. However, the effects of magnitude by light-limitation, nitrogen-limitation and phosphorus-limitation are different. In freshwater ecosystems, phosphorus-limitation is considered as a strongly driven factor that affects the phytoplankton growth and alters the community composition (Reeder et al., 2017), which is different from our result, where the light availability is the main driver of the phytoplankton proliferation because of higher TSS concentrations. The proportion of decreased diatoms with increasing N:P ratios and no significant change in green algae have been found in other aquatic ecosystems (Conley and Johnstone, 1995; Klausmeier et al., 2004; Torres-Águila et al., 2018). The shift in the predominant of N-fixing cyanobacteria (*Aphanizomenon*) in summer (May to July) to non-fixing cyanobacteria (*Microcystis*) in early fall (August to September) due to the change of its nitrogen and phosphorus cycles, has been found in Lake Utah (Li et al., 2020). Previous studies have shown that higher concentrations of P and lower N:P ratios favor of the N-fixing cyanobacterial blooms (Schindler, 1977; Smith, 1983, 1986; Havens et al., 2003; Vrede et al., 2009). As a fundamental energy source, light plays an important role in phytoplankton growth by promoting photosynthesis in the turbid water phase (higher TSS concentrations) (Gameiro et al., 2011; Curtarelli et al., 2015; Zou et al., 2020). Reducing available light can limit the uptake of N and P in phytoplankton and result in shifts in the species composition (Domingues et al., 2011; Jia et al., 2020). However, the roles of mechanisms and synergistic effects on the shifts in the phytoplankton communication composition under different prevailing environmental conditions have not been well studied. In addition, the outcome of the competition of the algal species may differ with respect to combination of nutrient ratios and co-varying environmental factors in different lakes (Teubner and Dokulil, 2002).

The numerical model is an effective tool to explore the driving factors of phytoplankton growth and depict a possible shift in phytoplankton community composition (Los and Wijsman, 2007; Los, 2009; Li et al., 2015). Various ecological models have been developed to describe nutrient competition for phytoplankton (Di et al., 1971; Smith, 1986; Zhang et al., 2003a; Zhang et al., 2003b; Wang et al., 2019). Based on the competition theory that the species with lowest "critical light intensity" are superior competitors, they can surpass other phytoplankton species and become dominant. Huisman et al. developed a competition model to predict the succession between buoyant and sinking phytoplankton species for light and reported that the cyanobacteria such as *Microcystis* and *Aphanizomenon* were better competitors than the green algae *Scenedesmus* under sufficient nutrients, and the same mixing layer and native species environmental conditions (Huisman et al., 1999; Huisman et al., 2004). A new coupled Euler-Lagrangian model has been used to explore the contribution of physiological and physical processes to the phenology of HABs in shallow lakes (Feng et al., 2018). However, traditional numerical models lack the process by which phytoplankton themselves interact with each other at species and phenotype levels and predict the long-term evolution of phytoplankton under co-varying environmental factors (Crisci et al., 2017; Wang and Zhang, 2020). Comprehensive modeling approaches integrated by hydrodynamic-ecological models have become popular for exploring phytoplankton growth and its driving factors in different cases (Zhang et al., 2013; Wang et al., 2019). These models can be effectively studied for the dynamic variation of primary products under different hydrodynamic and water quality conditions (Huang et al., 2012; Zhang et al., 2013). The Delft3D-BLOOM module, which is nested within the ecological model overcomes the defects of traditional models. This model can not only predict the fate and transport of pollutants, but also explore the phytoplankton species competition driven by co-varying conditions, thereby providing technical support for policymakers (Blauw et al., 2009; Wang et al., 2019). Process-based (PB) models are more frequently used to provide a comprehensive assessment of how environmental conditions such as physiological preferences, nutrient availability, vertical and horizontal transport, and mixing, affect the phytoplankton species competition in long-term predictions (hindcasting), whereas data-driven (DD) models (e.g., artificial neural networks, genetic programming, decision trees and Bayesian networks) can be employed for short-term forecasting of cyanobacterial blooms (Oliver et al., 2012; Fornarelli et al., 2013; Jiang et al., 2016; Rousso et al., 2020). The combination of the PB and DD models can improve the model performance in terms of model accuracy and computational efficiency (Wang et al., 2019). In this study, we intended to use a coupled hydrodynamic-ecological model (a nested ecological-phytoplankton bloom model) based on the Delft3D software suite to address phytoplankton succession and growth limitations under co-varying environmental conditions in a large shallow lake. Comapred to the previous modeling approaches, this study has the following features: 1. In the model structure, the bloom model consists of six phytoplankton functional groups or species, namely, diatoms, green algae, *Anabaena, Microcystis, Aphanizomenon* and *Oscillatoria*; each specie is further classified into N-limiting, P-limiting or L-limiting with different characteristics (e.g., different growth, mortality and respiration rates). Therefore, a total of 18 phytoplankton components at the taxonomic level can be simulated, and 2. In the model application, the succession and growth limitation of phytoplankton depends not only external co-varying environmental conditions such as light and nutrients, but also on the properties of species such as growth and mortality, as well as respiratory rates. Species competition is based on the trade-off principle between growth and environmental requirements through optimizing biomass using a linear program under constraints of the resources at the start of each time step, growth, and mortality rates.
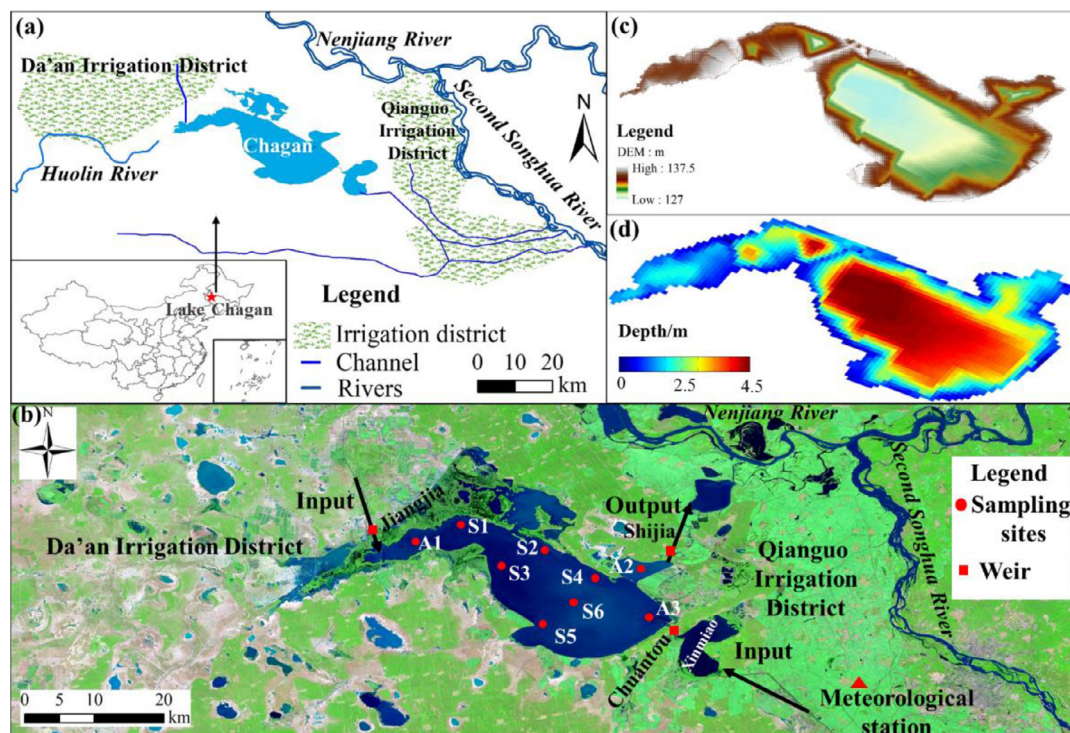
Fig. 1. Map of study area (a), Sampling sites (b), DEM (c) and Bathymetry (d) of Lake Chagan.

Lake Chagan is one of the ten largest freshwater lakes in China and is an important fishery base, which has been in a transition period from the clearwater phase to the turbid water phase as a result of receiving high concentrations of nutrients and TSS loading from the discharge of a new irrigation district (Da'an irrigation district) (Table S1; Liu et al., 2019). The gradual deterioration of water quality because of increasing levels of eutrophication in Lake Chagan has posed a potential serious threat to public and ecological health (Sun et al., 2014). Therefore, understanding the effect of the change in nutrients and TSS loadings driven by the new irrigation district development on the phytoplankton community structure and shift of dominant species compositions becomes important for the sustainable development of fisheries and water quality management. In addition, it could also explore why algae did not bloom in lakes with high concentrations of nutrient. It is hypothesized that i) higher TSS suppresses the growth of diatoms and green algae biomass but favors cyanobacteria dominance and ii) non-N-fixing cyanobacterial blooms would occur under higher N:P ratios and lower light intensities in the turbid water phase. The overall goal of this study is to comprehensively assess the effect of TSS and nutrients on phytoplankton dynamics and behaviors using a coupled hydrodynamic-ecological model in which a phytoplankton bloom was nested. In particular, this study aims to: i) reveal the spatiotemporal dynamics of phytoplankton species composition; ii) comprehensively quantify and reveal limiting factors influencing phytoplankton growth and succession; and iii) understand how changes in co-varying environmental conditions (e.g., N:P ratio, TN, TP and TSS concentrations) driven by the new irrigation district development would have a synergistic effect on the phytoplankton behaviors in the future.

2. Material and methods

2.1. Study area

Lake Chagan is located on the Songnen Plain of Northeast China (124°03′ - 124°34′E, 45°09′ - 45°30′N) (Fig. 1), with a surface area of 372 km^2 and an average water depth of 2.5 m. It is characterized by temperate continental monsoon semi-arid climate. The multi-year average evaporation, precipitation and temperature are 1449 mm, 400 mm and 4.5 °C, respectively (Fig. S1). The prevailing wind direction is southwest wind with the maximum wind speed of 27 m/s (Fig. S1).

Previous study has shown that the lake is at hypereutrophic status in summer (Liu et al., 2019). In addition to the contribution from precipitation and groundwater, the irrigation discharges from the Qianguo and Da'an irrigation district in the region serve as the main water inflow into the lake, together with the main outflow from Shijia weir and evaporation, influence the flow pattern in Lake Chagan (Zhang et al., 2017; Liu et al., 2020a; 2020b).

Lake Chagan is in the transition period from Class III of the National Surface Water Quality Standard of Chinese (clearwater phase) in 2011 to the Class V standard (turbid water phase) (Table S1). Based on the relationship between the average Secchi disk depth (SDD) and the total suspended solids (TSS), we defined that if the TSS concentrations are less than 60 mg/L (corresponding to SDD more than 46 cm), then it was in the clearwater phase, and the if the TSS concentrations exceed this concentration, then it was in the turbid water phase in Lake Chagan.

2.2. Sample collection and analysis

In this study, Lake Chagan was divided into three sampling fields, namely the western part (A1, S1), the middle part (S2-S5), and the eastern part (A2-A3, S6), with a total of nine sampling stations corresponding to physical parameter fields, such as flow and depth fields and general water quality parameter fields, such as TN and TP concentrations, respectively (Liu et al., 2020b) (Fig. 1). Among them, A1-A3 were outflow and inlet sampling stations, and S1-S6 were the sampling stations inside the lake. Water quality samples were collected monthly from May to October 2018 and May to September 2019 (Fig. 1 and Table S2). A total of 99 water samples were collected. Phytoplankton samples were collected monthly in May and September 2018. Atmospheric deposi-

tions of nitrogen and phosphorus concentrations were collected in this region in May and September 2018. Monthly sediment samples from Lake Chagan were collected in May and September 2018 using a Piston-type cylindrical mud dredger. Water quality samples of groundwater were collected in May and September 2018 (Liu et al., 2019). Water temperature (T_w), pH, electronic conductivity (EC) and secchi disk depth (SDD) were measured using a Hanna measurement probe on-the-spot and Secchi disk, respectively. Total nitrogen (TN), total phosphorus (TP), ammonia nitrogen (NH_4-N), nitrate nitrogen (NO_3-N), phosphate(PO_4^{3-}), TSS, chlorophyll-a (Chl-a) and dissolved oxygen (DO), as well as phytoplankton and zooplankton biomass data were analyzed at the Institute of Agricultural Ecology, Northeast Geography of the Chinese Academy of Sciences. The methodology used for the quantification of water quality parameters was shown in a previous study (Liu et al., 2019). Phytoplankton samples were preserved with Lugol's iodine solution (2% final conc.) and settled for 48 h before the analysis. Phytoplankton samples were obtained using No. 25 phytoplankton bionet (pore size of 64 μm) at 0.3 - 0.5 m below the water surface and slowly dragged in an "∞" shape for 3 min. The water in the bionet was then concentrated to 100 mL and fixed in 1 - 2 mL Lugol's iodine solution. One-liter samples were fixed in 10 mL Lugol's iodine solution and were concentrated to 50 mL with a siphon after sedimentation for 48 h, and 4% formaldehyde solution was added to save the mirror Check. The identification of phytoplankton species is based on the protocol in "Phytoplankton Handbook" (Hasle and Sournia, 1978) and "Chinese Freshwater Algae - System, Classification and Ecology" (Hu and Wei, 2006). The algal cell counts were measured by a 0.1 mL counting frame and performed under a microscope (Olympus CX21, 400x). Each sample was counted twice with 100 view fields each time, and the average value was used. The corresponding algal biomass was calculated based on the cell bio-volume for each individual species (Sun and Liu, 1999). The velocity and flow data were derived from the data of Lake Chagan at the automatic hydrological monitoring station. Meteorological data were obtained from the China Meteorological Science Data Center (https://data.cma.cn/). The TSS concentrations of Lake Chagan from May to October in 2011 and 2018 were retrieved from the Landsat eight remote sensing data from the U.S. Geological Survey (USGS) (https://earthexplorer.usgs.gov/). The equations describing the relationship between the remote sensing band and TSS were shown in Table S3. Detailed information on the calculation method are presented in Supplement document 1. The average TSS concentration in the lake in 2011 (59.89 mg/L) was significantly lower than the current average (147.67 mg/L). The analysis was based on the datasets from meteorological, hydrological, water quality, plankton, and remote sensing data. Detailed information related to specific parameters, time periods and corresponding data sources of the dataset are shown in Table S2.

2.3. A comprehensive framework for hydrodynamic-ecological modeling

2.3.1. Model setup

The comprehensive hydrodynamic-ecological model was built based on the Delft3D FLOW and WAQ modules (Fig. S2) to better understand how different environmental factors affect the changes in phytoplankton dynamics and behaviors in Lake Chagan. It consisted of a hydrodynamic module, an ecological module, and a nested phytoplankton bloom module (Fig. 2). The hydrodynamic module provides a physical transport process to the ecological module, which reflects complex interactions between different state variables such as phytoplankton and nutrients, TSS, and driving forces (e.g., wind and solar radiation) (Liu et al., 2020b). The Delft3D ecological module provides the nutritional foundation for the nested BLOOM module that describes the dynamics and behav-

ior of phytoplankton species. Detailed descriptions of the comprehensive model and governing equations are presented in Supplement document 2.

2.3.2. Modeling of phytoplankton growth limitation and species competition

Phytoplankton adapts to changing environmental conditions and continuously optimizes growth by reallocating nutrients and energy through metabolic pathways. Different phytoplankton taxa use different strategies to partition resources (Halsey et al., 2015). Hence, phytoplankton species can be further grouped into different limiting resource types. Based on the survey data, six phytoplankton functional groups, namely diatoms, green algae, *Anabaena, Microcystis, Aphanizomenon and Oscillatoria* were defined in the bloom model (Fig. S2). Each of the phytoplankton species are further divided into N-limited, P-limited and L-limited species (Blauw et al., 2009). Competition for nutrients and light resources not only occur between different phytoplankton functional groups, but also between different limited types of each species. Nitrogen types (N-limited) of phytoplankton were characterized by lower maximum growth rates, higher mortality rates, and higher Chl-a content, whereas phosphorus types (P-limited) of phytoplankton were also characterized by lower maximum growth rates and higher mortality rates but lower Chl-a content (Los and Brinkman, 1988; Los et al., 2008). In contrast, light types (L-limited) of phytoplankton were characterized by higher maximum growth rates and lower mortality rates (Los, 2005; Blauw et al., 2009). The bloom model aims to select the best adapted combination of phytoplankton types under different environmental constraints such as nutrients and light, growth and mortality limitations and grazing processes such as zooplankton (Los, 2009). It uses linear programming to maximize the total biomass of phytoplankton species at equilibrium under prevailing environmental conditions at each time step (Los and Brinkman, 1988). The model adopts a "conditional reallocation" scheme excluding all potential combinations of species which cannot be achieved within the time step size. Equations S18-S20 of each limiting type are presented in Supplement document 2.

2.3.3. Model input

Meteorological datasets, including hourly air temperature, precipitation, evaporation, relative humidity, solar radiation, wind direction, speed and cloud cover were used in 2018-2019 as inputs for building the hydrodynamic module. Integrated grid and bathymetry maps of the model domain are presented in Fig. 1. Detailed information on the hydrodynamic model setup in Lake Chagan can be found in Liu's previous study (Liu et al., 2020b). Total nitrogen (TN), total phosphorus (TP), ammonia nitrogen (NH_4-N), nitrate Nitrogen (NO_3-N), phosphate (PO_4^{3-}), total suspended solids (TSS), chlorophyll-a (Chl-a) and dissolved oxygen (DO), and phytoplankton and zooplankton biomass were used as the inputs for the WAQ-ECO model (e.g., from open boundaries at Chuantou weir, Jiangjia weir and Shijia weir). In addition, monthly water quality datasets from groundwater intrusion and atmospheric deposition were considered as additional model inputs. The model initial conditions and parameter coefficients used in the model are shown in Tables S4 and S5, respectively.

2.3.4. Model calibration and validation

The Delft3D-FLOW module, which provides the hydrodynamic foundation for the Delft3D-WAQ module, has been calibrated and validated using water temperature and salinity in the previous work (Liu et al., 2020b). Further calibration and validation were mainly focused on several key water quality parameters in the ecological model. The relevant state variables and processes as well as
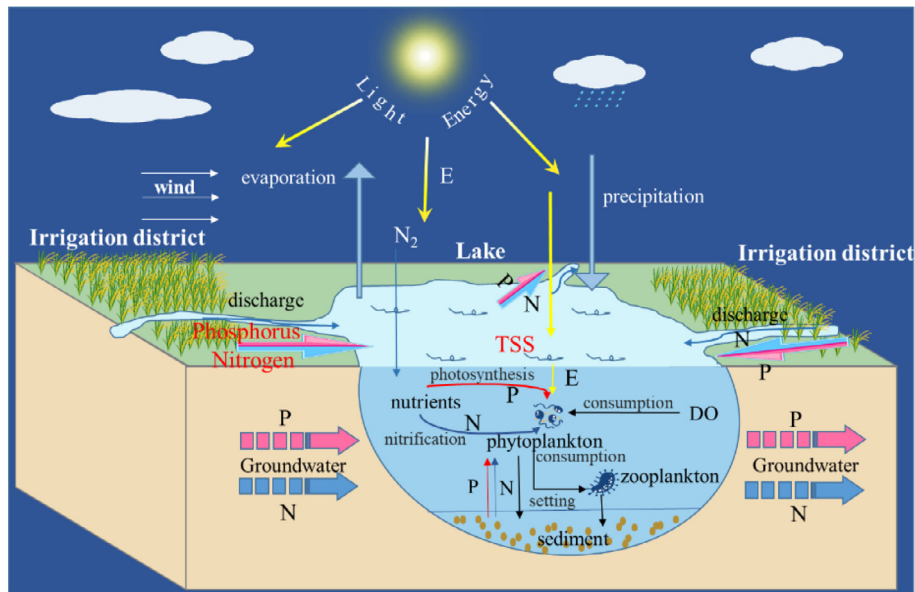
Fig. 2. The conceptual diagram of the comprehensive framework of phytoplankton bloom modeling

governing equations related to the comprehensive model are presented in Supplement document 2.

Datasets of TN, TP, DO, and Chl-a at nine observation stations from May to October, in 2018 and from May to September, in 2019 were used for the model calibration and validation, respectively. Owing to sparse data, the calibration and validation on the phytoplankton biomass were only based on the concentration of chlorophyll-a (Chl-a) and the dominant species. In addition to the visual inspection between modeled and observed values, we also quantified the model's performance based on different assessment criteria as shown in Table 2. Nash-Sutcliffe efficiency (NSE), root mean square error (RMSE) and average standard deviation (ARD%) were used to evaluate the model's performance. When the NSE is greater than 0.36, the performance of the model can be considered good and used for model application (Moriasi et al., 2007; Moriasi et al., 2015). The average standard deviation (ARD%) between simulated results and observations were results is also used to evaluate the model performance of the model. If the ARD% is less than 25%, the simulation results are considered satisfactory (Zhang et al., 2013; Xu et al., 2017).

Equations (1)-(3) are used for the evaluation:

$$NSE = 1 - \left[\frac{\sum_{i=1}^{n} \left(x_i^{obs} - x_i^{sim} \right)^2}{\sum_{i=1}^{n} \left(x_i^{obs} - x_i^{mean} \right)^2} \right] \qquad (1)$$

$$RMSE = \sqrt{\frac{1}{n} \sum_{i=1}^{n} (x_i - x_i)^2} \qquad (2)$$

$$ARD\% = \frac{\sum_{i=1}^{n} \left| X_i^{sim} - X_i^{obs} \right| / X_i^{obs}}{n} \qquad (3)$$

2.4. Scenario setup and analysis

In this study, five N:P ratios and two TSS concentrations, including the observed concentrations in the turbid water phase (average concentrations of TSS $\geq$ 60 mg/L) and inversion concentrations in the clearwater phase (average concentrations of TSS $\leq$ 60 mg/L), made a combination of 10 scenarios for the analysis and assessment (Tables 1 and S9). N:P ratios were tested with a value of either 5, 10, 15, 20 or 30 in the 10 scenarios. The corresponding

Table 1
Scenarios for testing impact of different driving factors on change of phytoplankton biomass and species composition.

Scenarios	N:P ratios	TN(mg/L)	TP(mg/L)	TSS(mg/L)	Status
1	N:P=10	Observed	Observed	Observed	Turbid water
2	N:P=10	Observed	Observed	Inversion	Clearwater
3	N:P=5	III (1.0)	IV (0.1)	Observed	Turbid water
4	N:P=5	III (1.0)	IV (0.1)	Inversion	Clearwater
5	N:P =15	IV (1.5)	IV (0.1)	Observed	Turbid water
6	N:P =15	IV (1.5)	IV (0.1)	Inversion	Clearwater
7	N:P =20	III (1.0)	III (0.05)	Observed	Turbid water
8	N:P =20	III (1.0)	III (0.05)	Inversion	Clearwater
9	N:P =30	IV (1.5)	III (0.05)	Observed	Turbid water
10	N:P =30	IV (1.5)	III (0.05)	Inversion	Clearwater

where III and IV represent the surface water classification criteria; "Observed" indicates the observed values of TN, TP, and TSS concentration; "Inversion" indicates the inversion value of TSS concentration in 2011.

concentrations of nutrients (TN and TP) and TSS were either derived from the measurements or based on the China's Environmental Quality III and IV Standards of Surface Waters (GB3838-2002) or from the inversion data. The detailed design of the 10 different combinations with specific values are shown in Tables S1 and S4 in Supplement document 3. In these scenarios, only the concentrations of TN, TP, and TSS were changed, and the flow rates remained unchanged. Scenarios 1 and 2 were the current states referring to the turbid water and the clearwater phase in Lake Chagan, respectively. They were chosen as the baselines to compare with other scenarios and study the synergistic impact of TSS, TN, TP and N:P ratios on phytoplankton dynamics and behaviors.

3. Results

3.1. Results of calibration and validation

The model performances are shown in Table 2 and Fig. S3. The NSE values at all observation stations were mostly 0.36 to 0.60, suggesting that the model yielded very good agreement between the observed and predicted results at each observation station. Given the sparse dataset, the model evaluation for predicting phytoplankton was based on comparing the simulated proportions with the observed values among the three mainly dominant groups

Table 2
Results of model calibration and validation.

Parameter	Indicator	Content	A1	A2	A3	S1	S3	S6
TN	*NSE*	C	0.33	0.12	0.28	0.37	0.13	0.28
		V	0.52	0.12	0.46	0.49	0.17	0.36
	RMSE	C	1.06	0.97	0.97	1.22	1.07	0.95
		V	1.28	1.12	1.08	1.49	1.19	1.11
	ARD%	C	7	9	16	10	15	18
		V	5	8	10	7	12	14
TP	*NSE*	C	0.38	0.24	0.27	0.13	0.26	0.25
		V	0.50	0.26	0.35	0.35	0.44	0.37
	RMSE	C	0.03	0.02	0.01	0.02	0.02	0.02
		V	0.05	0.02	0.01	0.04	0.03	0.03
	ARD%	C	8	11	18	9	14	17
		V	4	8	12	7	11	12
DO	*NSE*	C	0.45	0.28	0.03	0.32	0.61	0.31
		V	0.46	0.36	0.12	0.54	0.31	0.46
	RMSE	C	1.58	1.38	1.46	1.55	1.31	1.42
		V	1.68	1.54	1.56	1.67	1.48	1.53
	ARD%	C	8	15	16	18	10	22
		V	6	12	14	16	8	18
Chl-a	*NSE*	C	0.34	0.26	0.13	0.22	0.16	0.32
		V	0.59	0.31	0.39	0.49	0.25	0.46
	RMSE	C	1.13	1.04	1.42	1.11	1.07	0.99
		V	1.87	1.52	1.67	1.17	1.46	1.19
	ARD%	C	5	10	18	8	15	24
		V	3	8	14	6	14	22
Cyanobacteria	ARD%	——	12	14	13	19	20	18
Green algae	ARD%	——	9	8	10	14	16	17
Diatoms	ARD%	——	10	8	9	12	13	15

Note: "C" represents calibration; "V" represents validation.

(i.e., cyanobacteria, green algae and diatoms) as shown in Fig. S4. All the ARD% values between the simulated and observed values were less than 25% and the validation results were greater than the results of calibration in all the indicators (Table 2).

3.2. Spatial-temporal dynamics of phytoplankton biomass and species succession

Based on the results of the baseline simulations in the turbid water phase, phytoplankton biomass in the wet season (June-September) was significantly higher than that in the dry season (May and October) (Fig. 3a). Species compositions of the phytoplankton in Lake Chagan were mainly diatoms, green algae, and cyanobacteria (Fig. 3b). Cyanobacteria of Lake Chagan mainly included N-fixing cyanobacteria (*Anabaena* and *Aphanizomenon*) and non-N-fixing cyanobacteria (*Microcystis* and *Oscillatoria*). The biomass proportion of non-N-fixing cyanobacteria was higher than that of N-fixing cyanobacteria (Fig. 3c).

The results showed that there was an obvious spatial heterogeneity of the average phytoplankton biomass during both the dry and wet seasons in 2018-2019 (Fig. 4). The phytoplankton biomass in Lake Chagan in the dry season showed an increasing trend from the western to eastern part, but the opposite pattern was observed during the wet season. Phytoplankton biomass in the wet season varied widely, with higher biomass than that in the turbid water phase.

3.3. Impact of limitations of nutrients and light on phytoplankton growth and succession

As shown in Fig. 5, the baseline results from the model simulations demonstrated that the growth of *Anabaena, Microcystis, Aphanizomenon, Oscillatoria*, diatoms, and green algae were severely limited by light, followed by nitrogen and phosphorus (with severe levels of L-limited > N-limited > P-limited) in Lake Chagan. The L-limited type of biomass of six phytoplankton functional groups, namely diatoms, green algae, *Anabaena, Microcystis, Aphanizomenon*, and *Oscillatoria* distributed the entire lake surface layer at approximately 0.3 - 0.5 m and accounted for approximately 50% of the total phytoplankton biomass proportion. The proportions of N-limited and P-limited types were similar in *Anabaena*, diatoms, green algae, *Microcystis* and *Aphanizomenon*, which accounted for approximately 25% of the total biomass. In contrast, the proportion of N-limited type (approximately 37%) of *Oscillatoria* was higher than that of P-limited type (approximately 23%). The P-limited proportion of phytoplankton was lower in the dry season (May and October).

3.4. Change of phytoplankton biomass and shifts of dominant species under prevailing environmental conditions

The simulated results of monthly variations in the influence of N:P ratios and concentrations of TN, TP, and TSS on phytoplankton biomass are shown in Fig. 6. In general, phytoplankton biomass was lower in the turbid water phase than in the clearwater phase when the concentrations of TN and TP remained unchanged. Phytoplankton biomass rapidly increased with decreasing TSS in eutrophic water (higher TN and TP). In contrast, the impact was less in the oligotrophic water (lower TN and TP). Variations in N:P ratios had little effect on the change in the phytoplankton biomass in the turbid water phase. Maximum phytoplankton biomass was observed in Scenarios 7 and 8 and minimum phytoplankton biomass was observed in Scenarios 1 and 2 in the baseline approaches.

Fig. 7 shows the monthly variations of the predicted impacts on the changes in N:P ratios and concentrations of TN, TP, and TSS on phytoplankton dynamic competition and succession. The biomass proportion of green algae was dominant under higher light intensities (lower TSS) in late summer when compared to the opposite pattern of the dominance of diatoms and non-N- cyanobacteria in early summer and fall (Fig. 7). The biomass proportion of N-fixing cyanobacteria (*Anabaena* and *Aphanizomenon*) was lower than non-N-fixing cyanobacteria (*Microcystis* and *Oscillatoria*) un-
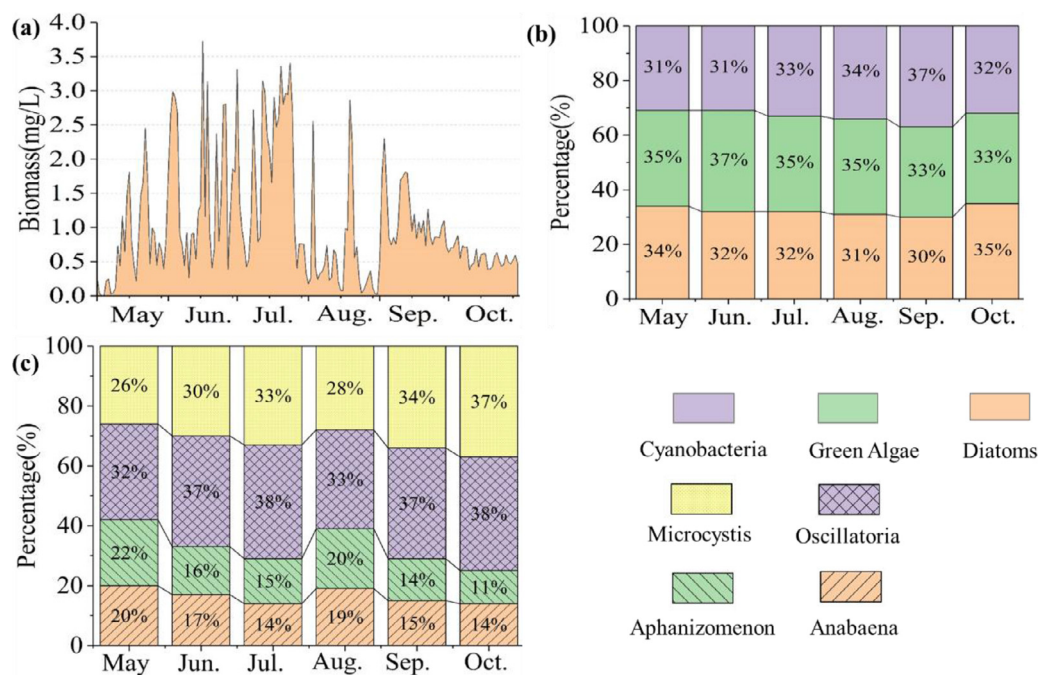
Fig. 3. Monthly average variation of phytoplankton species and biomass in Lake Chagan between May and October in 2018-2019; (a) The total biomass of phytoplankton; (b) The percentages of main phytoplankton group species; (c) The percentage of cyanobacteria species
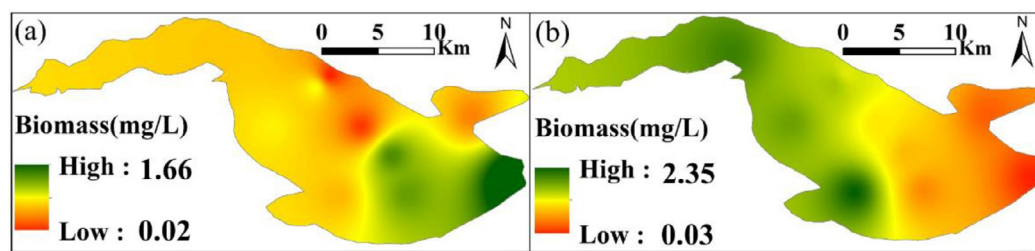

Fig. 4. Spatial distribution of averaged phytoplankton in Lake Chagan: (a) in the dry season May and October; and (b) in the wet season including June, July, August, and September during 2018-2019.

Table 3
Phytoplankton succession and proportions of predominant species in the ten different scenarios in Lake Chagan.

Group	1	2	3	4	5	6	7	8	9	10
Cyanobacteria (%)	28	28	28	27	29	29	46	34	34	30
Green algae (%)	36	33	36	33	34	34	27	32	32	35
Diatoms (%)	34	39	36	40	37	37	27	34	34	35

der the same nutrient concentrations in the turbid water phase. It was also observed that the biomass proportion of cyanobacteria increased with increasing N:P ratios when the N:P ratios exceeded the 20. The biomass proportion of N-fixing cyanobacteria was higher than non-N-fixing cyanobacteria when the N:P ratios was less than 20, whereas the biomass proportion of non-N-fixing cyanobacteria was higher than that of N-fixing cyanobacteria when the N:P ratios exceeded 20. Cyanobacteria became dominant when N:P ratios were close to 20 in the turbid water phase (Table 3).

The secchi disk depth (SDD) increased from May to September and decreased from September to October in both the clearwater and turbid water phases (Fig. 8). The change in SDD values in the turbid water phase was lower than the clearwater phase. The SDD was less than 46 cm in the turbid water phase, and from 46 cm onwards in the clearwater phase, respectively. It is interesting that N:P ratios had little effect on the changes in SDD values.

4. Discussion

4.1. Impact of driving force on phytoplankton growths and dynamics

Phytoplankton biomass in Lake Chagan showed obviously spatiotemporal heterogeneity with increasing TN, TP and TSS concentration (Fig. 3-4). Extensive studies have shown that nutrient (nitrogen, phosphorus) and light were the main resources for phytoplankton reproduction (Cloern, 1999; Klausmeier et al., 2004; Søndergaard et al., 2017). Excess nutrient inputs can result in lake eutrophication (Smith et al., 1999; Smith and Schindler, 2009). Higher concentrations of nutrients and suspended solids carried by the new irrigation discharge have been the main pollution sources in Lake Chagan (Fig. S6 and Liu et al., 2020a). In both the turbid and the clearwater phase, light can be the main limiting factor for phytoplankton growth when compared to N and P availability due to higher TSS concentrations blocking the light penetra-
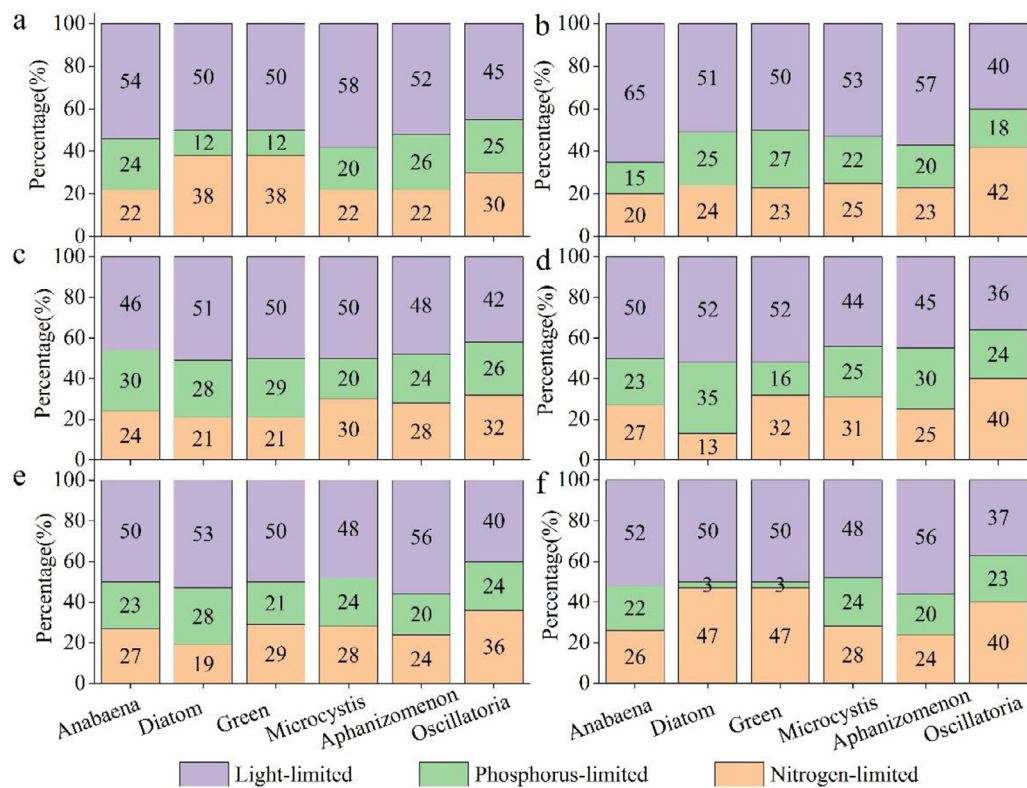
Fig. 5. Monthly variation of the proportions (%) of nitrogen (N)-, phosphorus (P)-, light (L)-limiting types of different phytoplankton functional groups, where "a to f" refers to May, June, July, August, September, and October, respectively.
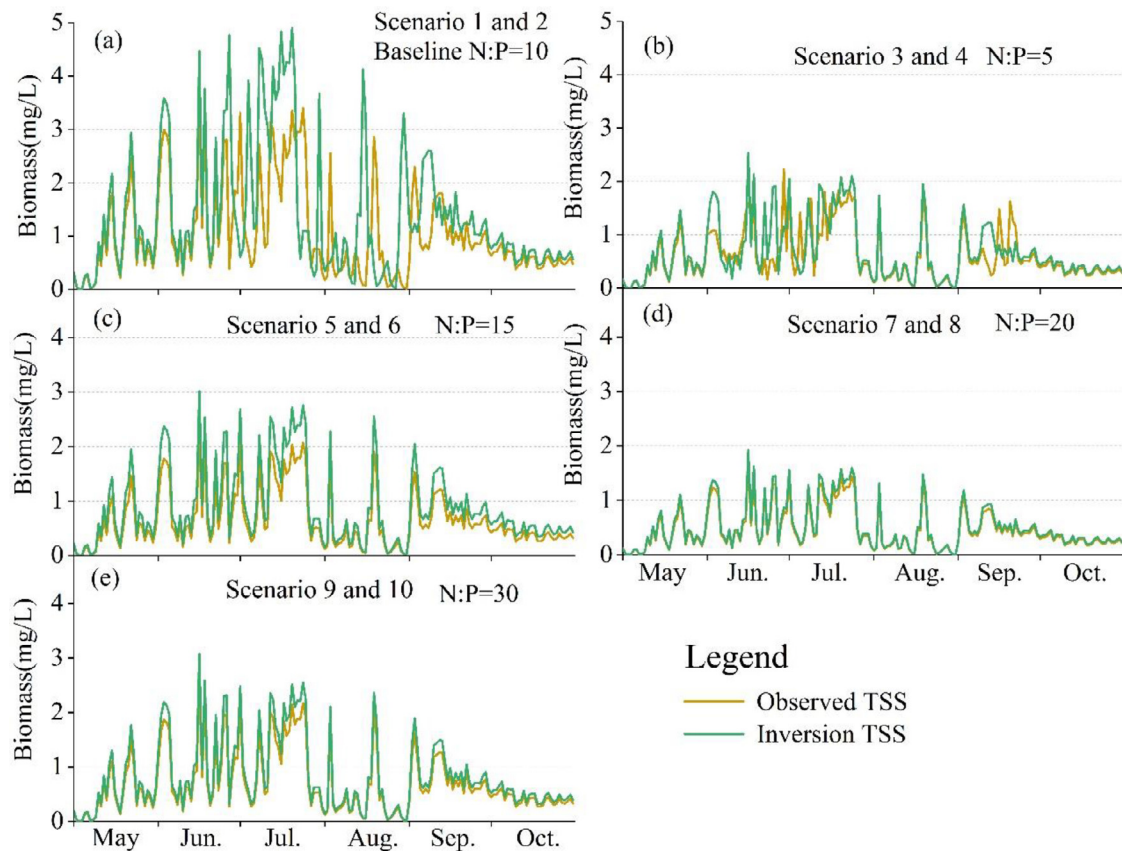

Fig. 6. Monthly variation of simulated phytoplankton biomass under 10 Scenarios. The orange line and green line illustrate the dynamics of phytoplankton biomass under the scenarios corresponding to the TSS concentrations in the observed values and the inversion values, respectively. The higher observed TSS concentrations indicate the turbid water phase and the lower inversion TSS concentrations indicate the clearwater phase.
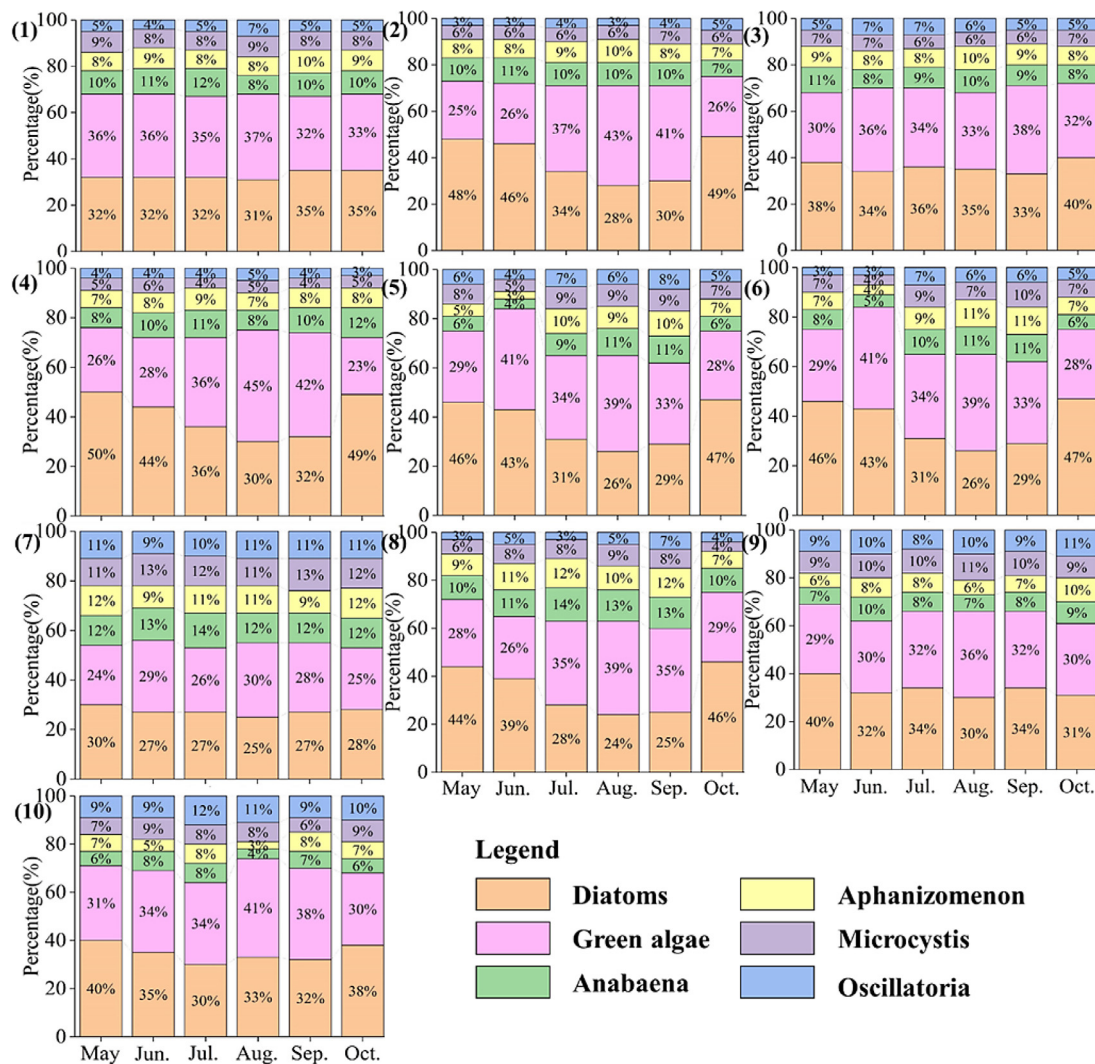
Fig. 7. Monthly variations of the simulated phytoplankton species proportions in 10 scenarios

tion into the water column (Gameiro et al., 2011; Domingues et al., 2011). Our results demonstrated that phytoplankton growth in Lake Chagan was mainly limited by light intensities, which accounted for approximately 50% of the total phytoplankton biomass (Fig. 5). Higher TSS concentrations not only influence the photosynthesis of phytoplankton (Hoyer and Jones, 1983; Jones and Knowlton, 2005; Dzialowski et al., 2011; Liu et al., 2016), but also change the nitrogen and phosphorus cycle absorbing NH_4-N and dissolved inorganic phosphorus (DIP) in the water body, thereby inhibiting the uptake of nitrogen and phosphorus in phytoplankton (House et al., 1995; Wollheim et al., 2001; Smith et al., 2005; Ekka et al., 2006). Therefore, phytoplankton biomass showed an increasing trend with increasing nutrient (N and P) concentrations and decreased TSS concentration from May to July (Figs. 3, S5, and S6).

The concentrations of TSS in clearwater are less than 60 mg/L and the concentrations of TSS in turbid water are more than 60 mg/L. Phytoplankton biomass in the turbid water phase decreased from the western to the eastern part with increasing TSS concentrations in the dry season (Fig. 4). The TSS in this study included inorganic suspended solids (ISS) and organic suspended solids (OSS). Phytoplankton and detritus are part of the OSS that come from the internal contribution of the lake. TSS can inhibit the growth of phytoplankton through light limitation and thereby reduce the OSS concentration to some extent. The field study re-

sults at nine sampling stations in May 2019 demonstrated that the ISS/TSS ratios ranged from 60 to 86%, suggesting that the ISS was the main contributor to the total suspended solids in the lake (Fig. S8). In addition, the modeled result also shows that the contribution from phytoplankton was very small (total biomass less than 5.0 mg C/L) when compared to higher ISS concentrations. The increase in TSS was not because of blooms, but originated from inorganic terrestrial inputs (Li et al., 2016). Therefore, reducing the input of inorganic suspended solids from irrigation districts is beneficial for improving lake water quality. Because most of the ISS input came from the catchment area, we can argue that the external loading of ISS plays a vital role in suppressing the growth of diatoms and green algae but favoring cyanobacteria dominance, particularly in turbid water. To explore the impact of TSS on the change of water status, we also plotted TSS against the change of SDD in both clearwater and turbid water, based on the definition of the threshold (60 mg/L corresponding to 46 cm of Secchi disk depth (SDD)) in Chagan as shown in Fig.S9. The N:P ratios in the clearwater phase had a significant impact on the change in phytoplankton biomass (Hegarty and Villareal, 1998; Klausmeier et al., 2004). This is consistent with our finding that the difference in phytoplankton biomass between different scenarios under different N:P ratios were larger in the clearwater phase (Fig. 7). In addition, the concentrations of nitrogen and phosphorus were the main lim-
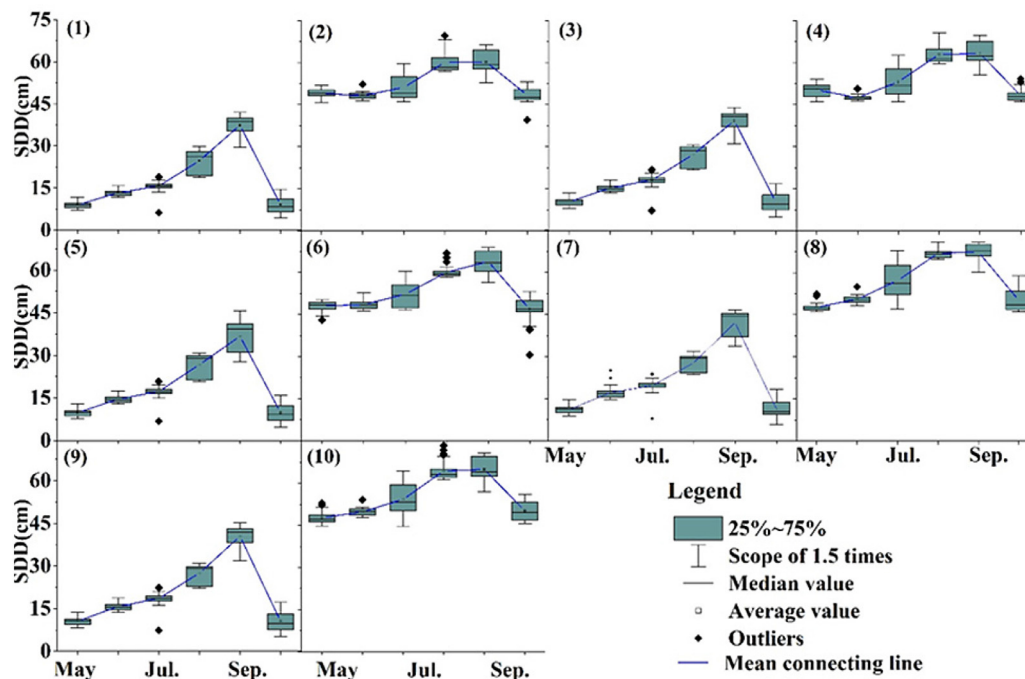
Fig. 8. Monthly variations of simulated SDD (secchi disk depth) values in 10 scenarios

iting factors of phytoplankton growth biomass when compared to the N:P ratios in the turbid water phase (Fig. 7). Hence, short-term alone management of N:P ratios was unlikely to effectively control algal blooms than dual N and P reductions, and it should also be combined with other impacts from the co-varying environmental conditions (Chislock et al., 2014).

4.2. Shifts of phytoplankton assemblages driven by co-varying environmental factors

Species competition played a vital role in the formation of HABs (Su et al., 2017; Li et al., 2020), which was affected by N:P ratios and concentrations of TN, TP, and TSS. Heterogeneity affected the interspecies competition of phytoplankton by influencing the growth of other coexisting algae and feeding of zooplankton, thereby gaining a competitive advantage (Gross and Yellen, 2003; Graneli et al., 2008). Green algae growth could be promoted by higher light intensities, while N:P ratios had little effect on it (Sorokin and Krauss, 1958; Solovchenko et al., 2008; Béchet et al., 2013). Because diatoms were relatively weaker competitors in the water environment with insufficient phosphorus supply (high N:P ratios) (Torres-Águila et al., 2018), lower N:P ratios and higher light intensities were in favor of N-fixing cyanobacteria in the clearwater phase (Fig. 7). N-fixing cyanobacteria would be limited by lower light intensities in the turbid water phase because there may not be enough energy to maintain N-fixation (Havens et al., 2003; Agawin et al., 2007; de Tezanos Pinto, P and Litchman, 2010a and 2010b). Previous studies have shown that higher N:P ratios and lower light intensities were in favor of the non-N-fixing cyanobacteria in the turbid water phase (de Tezanos Pinto and Litchman, 2010b; Carey et al., 2012; Chislock et al., 2014; Scott, et al., 2019). Hence, we might observe non-N-fixing cyanobacterial dominant under high N:P ratios because of the overriding effect of L-limited in the turbid water phase (Fig. 7). The toxins released by non-N-fixing cyanobacteria including *Microcystis* and *Oscillatoria* can jeopardize ecosystem functioning and threaten human health (Utkilen and Gjølme, 1995; Ziegmann et al., 2010; Horst et al., 2014). The results of this study revealed that the proposition of

predominant cyanobacteria showed a dynamic change along the N:P ratio gradient in Lake Chagan. Previous studies have shown that cyanobacteria tend to dominate when N:P ratios do not exceed 29 in natural water bodies (Smith, 1983; Paerl et al., 2001; Liu et al., 2011). In this study, the community shifts from diatoms and green algae to cyanobacteria along with the increasing N:P ratios until 20 in the turbid water phase (Fig. 7 and Table 3). In general, lower N:P ratios and lower light intensities are not favorable for non-N-fixing cyanobacteria (Teubner and Martin, 2002; de Tezanos Pinto and Litchman, 2010a; 2010b). Cyanobacteria have no obvious competitive advantage when the N:P ratios are close to the Redfield ratio (N:P ratio = 16) in the turbid water phase (Redfield, 1958). The biomass proportion of diatoms and green algae increased and that of cyanobacteria decreased when N:P ratios were less than 20, particularly in the clearwater phase (Table 3). These results have confirmed the hypothesis that cyanobacterial blooms would occur in the turbid water phase

Under co-varying environmental conditions, different types of N-fixing cyanobacteria have obvious differences in competitiveness, such as *Anabaena* and *Aphanizomenon*, although *Aphanizomenon* has a broader absorption spectrum and its growth is less limited by light than that of *Anabaena* (Agawin et al., 2007). In contrast, *Anabaena* has a higher growth rate than *Aphanizomenon* (Carey et al., 2012). Therefore, *Anabaena* was found to be more competitive than *Aphanizomenon* under lower N:P ratios and higher TSS concentrations when both species coexisted in the natural water bodies as shown in Fig. 7. The higher proportions of non-N-fixing cyanobacteria than those of N-fixing cyanobacteria when the N:P ratios exceeded 20, also confirmed our second hypothesis that non-N-fixing cyanobacterial blooms would occur under higher N:P ratios and lower light intensities in the turbid water phase.

4.3. Strategies of planning and management of water quality

Reducing the external pollution loading into aquatic ecosystems, dredging, and water diversion have become important measures for controlling the proliferation of cyanobacterial blooms and restoration of lake ecosystems (Newcombe et al., 2012; Lürling and

Faassen, 2012; Schindler et al., 2016; Dai et al., 2020). Our findings demonstrated that lower light intensities decreased total phytoplankton biomass but increased the proportion of cyanobacterial biomass (Fig. 6, Fig. 7, and Table 3). In addition, lower nutrient concentrations do not favor cyanobacterial blooms (Schindler et al., 2016; Dai et al., 2020). Improving the purification capacity of pre-wetlands in lakes (Yang et al., 2015), reducing the pollution from external point and non-point sources (Guo et al., 2014), and diluting water by water diversion projects (Zhu et al., 2008; Feng and Zhao, 2020) can effectively reduce the concentration of nitrogen and phosphorus in the water bodies. Lower light intensities do not favor phytoplankton growth but can lead to a shift in the phytoplankton community to cyanobacterial dominance. In order to sustain good ecological status in the lake, we recommend that TN, TP and TSS concentrations in the lake should be maintained or below a threshold level (TN $\leq$ 1.5 mg/L; TP $\leq$ 0.1 mg/L; N:P ratios between 15 and 20; and TSS $\leq$ 60 mg/L) (Fig. S6 and Fig. S7).

4.4. Impact of data frequency on analysis of environment conditions

The model performance is always dependent on how well the model is calibrated and validated, which requires sufficient amounts and quality of the available data (Zhang et al., 2003b; Wang et al., 2019). Therefore, the impact of data frequency used in the model should be taken into consideration. General water quality models are calibrated with data from a monitoring program that samples the environmental conditions at monthly base, allowing the simulation to reproduce seasonal and annual variations (Kara et al., 2012; Xu et al., 2017). However, compared with the water quality models, the ecological models in general need to describe the dynamics of phytoplankton in rapid water pollution events, which are often limited by the frequency of observed data (Kara et al., 2012; Huisman et al., 2019). Low frequency may limit our understanding of the actual dynamics and prevent capture of real behavior (Jørgensen and Bendoricchio, 2001). Data frequency has relatively little impact on the predicted nitrogen and phosphorus concentrations in water bodies (Bowes et al., 2016). The high-frequency input data (e.g., hourly meteorological data and flow data) can improve the accuracy of the hydrodynamic module as shown in our case study. The hourly output of the hydrodynamic module has been used as the input to the nested ecological model in this study. The integrated process-based hydrodynamic-ecological model was applied to quantify and predict the influence of environmental conditions on phytoplankton growth and succession in the seasonal and annual scale simulation and yielded reasonable results (Figs. 6 and 7). Likewise, the challenges of impacts of sparse and low-frequency datasets on the model calibration have existed in this study. The impact of vertical migration of cyanobacteria on phytoplankton dynamics was not considered in this study, which is limited by the available data. It is expected that high-frequency surveys of phytoplankton species and other water quality parameters (e.g., hourly, weekly, daily base or combination with online-sensor data), especially during the bloom period, will improve the model performance. The high-frequency datasets can also help improve the PB forecasting accuracy of phytoplankton when combined with the data-driven model (Wang et al, 2019). Thus, a further improvement of the accuracy and forecasting capacity of the integrated hydrodynamic-ecological model (PB) can be combined with high-frequency data survey and data-driven model (DD) in our future work.

5. Conclusions

Based on the simulated results of the dynamics of phytoplankton communities under different nutrient (TN and TP) levels and total suspended solid (TSS) concentrations in Lake Chagan using

the hydrodynamic-ecological modeling, it was found that phytoplankton growth was limited by light intensities and nutrient availability in the turbid water phase. Light limitation was the primary factor determining phytoplankton production and changes in the community structure. The order of limiting importance was in the form of L-limitation > N-limitation > P-limitation. The limitation and competition for nutrients and light affected the spatiotemporal distribution of phytoplankton in this large shallow lake. The phytoplankton community shifted from diatoms and green algae to non-N-fixing cyanobacteria with a higher N:P ratio and higher TSS (more than 60 mg/L) in the turbid water phase (SDD less than 46 cm). Lower light intensities limited the energy required to maintain N-fixation of N-fixing cyanobacteria under lower N:P ratios. These findings support our initial hypothesis that TSS suppresses the total diatoms and green algae biomass but favores the dominance of cyanobacteria in the turbid water phase, and non-N-fixing cyanobacterial blooms would occur under higher N:P ratios and lower light intensities in the turbid water phase. This study provides a better understanding of the role and mechanisms of phytoplankton growth and competition for resources under co-varying environmental conditions and provides useful information for policymakers in the control of cyanobacteria blooms and socio-ecological stability along a gradient of irrigation development.

Declaration of Competing Interest

The authors declare that they have no conflict of interest.

CRediT authorship contribution statement

Xuemei Liu: Conceptualization, Methodology, Software, Data curation, Writing - review & editing. **Liwen Chen:** Methodology, Data curation, Writing - review & editing. **Guangxin Zhang:** Conceptualization, Writing - review & editing, Funding acquisition. **Jingjie Zhang:** Methodology, Software, Writing - review & editing, Funding acquisition. **Yao Wu:** Data curation. **Hanyu Ju:** Data curation.

Acknowledgements

Supplementary materials

Supplementary material associated with this article can be found, in the online version, at doi:10.1016/j.watres.2021.116910.

References

Abell, J.M., Özkundakci, D., Hamilton, D.P., 2010. Nitrogen and phosphorus limitation of phytoplankton growth in New Zealand lakes: implications for eutrophication control. Ecosystems 13 (7), 966–977.

Agawin, N.S., Rabouille, S., Veldhuis, M.J., Servatius, L., Hol, S., van Overzee, H.M., Huisman, J., 2007. Competition and facilitation between unicellular nitrogen–fixing cyanobacteria and non-nitrogen-fixing phytoplankton species. Limnology and Oceanography 52 (5), 2233–2248.

Assemany, P.P., Calijuri, M.L., do Couto, E.D.A., de Souza, M.H.B., Silva, N.C., da Fonseca Santiago, A., de Siqueira Castro, J., 2015. Algae/bacteria consortium in high rate ponds: influence of solar radiation on the phytoplankton community. Ecological Engineering 77, 154–162.

Axler, R.P., Redfield, G.W., Goldman, C.R., 1981. The importance of regenerated nitrogen to phytoplankton productivity to phytoplankton productivity in a subalpine lake. Ecology 62 (2), 345–354.

Béchet, Q., Shilton, A., Guieysse, B., 2013. Modeling the effects of light and temperature on algae growth: state of the art and critical assessment for productivity prediction during outdoor cultivation. Biotechnology Advances 31 (8), 1648–1663.

Blauw, A.N., Los, H.F., Bokhorst, M., Erftemeijer, P.L., 2009. GEM: a generic ecosystems model for estuaries and coastal waters. Hydrobiologia 618 (1), 175.

Bowes, M.J., Loewenthal, M., Read, D.S., Hutchins, M.G., Prudhomme, C., Armstrong, L.K., Carvalho, L., 2016. Identifying multiple stressor controls on phytoplankton dynamics in the River Thames (UK) using high-frequency water quality data. Science of the Total Environment 569, 1489–1499.

Boyer, J.N., Kelble, C.R., Ortner, P.B., Rudnick, D.T., 2009. Phytoplankton bloom status: Chlorophyll a biomass as an indicator of water quality condition in the southern estuaries of Florida. USA. Ecological Indicators 9 (6), S56–S67.

Carey, C.C., Ibelings, B.W., Hoffmann, E.P., Hamilton, D.P., Brookes, J.D., 2012. Eco-physiological adaptations that favour freshwater cyanobacteria in a changing climate. Water Research 46 (5), 1394–1407.

Chislock, M.F., Sharp, K.L., Wilson, A.E., 2014. Cylindrospermopsis raciborskii dominates under very low and high nitrogen-to-phosphorus ratios. Water Research 49, 207–214.

Cloern, J.E., 1999. The relative importance of light and nutrient limitation of phytoplankton growth: a simple index of coastal ecosystem sensitivity to nutrient enrichment. Aquatic Ecology 33 (1), 3–15.

Conley, D.J., Johnstone, R.W., 1995. Biogeochemistry of N, P and Si in Baltic Sea sediments: response to a simulated deposition of a spring Diatoms bloom. Marine Ecology Progress Series 122, 265–276.

Crisci, C., Terra, R., Pacheco, J.P., Ghattas, B., Bidegain, M., Goyenola, G., Mazzeo, N., 2017. Multi-model approach to predict phytoplankton biomass and composition dynamics in a eutrophic shallow lake governed by extreme meteorological events. Ecological Modelling 360, 80–93.

Curtarelli, M.P., Ogashawara, I., Alcântara, E.H., Stech, J.L., 2015. Coupling remote sensing bio-optical and three-dimensional hydrodynamic modeling to study the phytoplankton dynamics in a tropical hydroelectric reservoir. Remote Sensing of Environment 157, 185–198.

Dai, J., Wu, S., Wu, X., Lv, X., Sivakumar, B., Wang, F., Yu, L., 2020. Impacts of a large river-to-lake water diversion project on lacustrine phytoplankton communities. Journal of Hydrology, 124938.

de Tezanos Pinto, P., Litchman, E., 2010a. Eco-physiological responses of nitrogen–fixing cyanobacteria to light. Hydrobiologia 639 (1), 63–68.

de Tezanos Pinto, P., Litchman, E., 2010b. Interactive effects of N: P ratios and light on nitrogen-fixer abundance. Oikos 119 (3), 567–575.

Di Toro, D.M., O'CONNOR, D.J., Thomann, R.V., 1971. A dynamic model of the phytoplankton population in the Sacramento San Joaquin Delta. Advances in Chemistry Services 106, 131–180.

Diatta, J., Waraczewska, Z., Grzebisz, W., Niewiadomska, A., Tatuśko-Krygier, N., 2020. Eutrophication induction via N:P and P/N ratios under controlled conditions—effects of temperature and water sources. Water, Air, Soil Pollution 231 (4), 1–18.

Domingues, R.B., Anselmo, T.P., Barbosa, A.B., Sommer, U., Galvão, H.M., 2011. Light as a driver of phytoplankton growth and production in the freshwater tidal zone of a turbid estuary. Estuarine, Coastal and Shelf Science 91 (4), 526–535.

Dzialowski, A.R., Smith, V.H., Wang, S.H., Martin, M.C., Jr, F.D., 2011. Effects of non-algal turbid on cyanobacterial biomass in seven turbid Kansas reservoirs. Lake and Reservoir Management 27 (1), 6–14.

Ekka, S.A., Haggard, B.E., Matlock, M.D., Chaubey, I., 2006. Dissolved phosphorus concentrations and sediment interactions in effluent–dominant Ozark streams. Ecological Engineering 26 (4), 375–391.

Faithfull, C.L., Bergström, A.K., Vrede, T., 2011. Effects of nutrients and physical lake characteristics on bacterial and phytoplankton production: A meta-analysis. Limnology and Oceanography 56 (5), 1703–1713.

Feng, D., Zhao, G., 2020. Footprint assessments on organic farming to improve ecological safety in the water source areas of the South-to-North Water Diversion project. Journal of Cleaner Production 254, 120130.

Feng, T., Wang, C., Wang, P., Qian, J., Wang, X., 2018. How physiological and physical processes contribute to the phenology of cyanobacterial blooms in large shallow lakes: A new Euler-Lagrangian coupled model. Water Research 140, 34–43.

Fornarelli, R., Galelli, S., Castelletti, A., Antenucci, J.P., Marti, C.L., 2013. An empirical modeling approach to predict and understand phytoplankton dynamics in a reservoir affected by interbasin water transfers. Water Resources Research 49 (6), 3626–3641.

Gameiro, C., Zwolinski, J., Brotas, V., 2011. Light control on phytoplankton production in a shallow and turbid estuarine system. Hydrobiologia 669 (1), 249.

Glibert, P.M., Burkholder, J.M., 2011. Harmful algal blooms and eutrophication: "strategies" for nutrient uptake and growth outside the Redfield comfort zone. Chinese Journal of Oceanology and Limnology 29 (4), 724–738.

Graneli, E., Weberg, M., Salomon, P.S., 2008. Harmful algal blooms of allelopathic microalgal species: the role of eutrophication. Harmful Algae 8 (1), 94–102.

Gross, J.L., Yellen, J. (Eds.), 2003. Handbook of graph theory. CRC press.

Guo, W., Fu, Y., Ruan, B., Ge, H., Zhao, N., 2014. Agricultural non-point source pollution in the Yongding River Basin. Ecological Indicators 36, 254–261.

Halsey, Kimberly, H., Bethan, M., Jones, 2015. Phytoplankton strategies for photosynthetic energy allocation. Annual Review of Marine Science 7, 265–297.

Hasle, G., Sournia, A., 1978. Phytoplankton Manual, Monographs on Oceanographic Methodology. UNESCO, Paris.

Havens, K.E., James, R.T., East, T.L., Smith, V.H., 2003. N:P ratios, light limitation, and cyanobacterial dominant in a subtropical lake impacted by non-point source nutrient pollution. Environmental Pollution 122 (3), 379–390.

Hegarty, S.G., Villareal, T.A., 1998. Effects of light level and N: P supply ratio on the competition between Phaeocystis cf. pouchetii (Hariot) Lagerheim (Prymnesiophyceae) and five Diatoms species. Journal of Experimental Marine Biology and Ecology 226 (2), 241–258.

Horst, G.P., Sarnelle, O., White, J.D., Hamilton, S.K., Kaul, R.B., Bressie, J.D., 2014. Nitrogen availability increases the toxin quota of a harmful cyanobacterium, Microcystis aeruginosa. Water Research 54, 188–198.

House, W.A., Denison, F.H., Armitage, P.D., 1995. Comparison of the uptake of inorganic phosphorus to a suspended and stream bed-sediment. Water Research 29 (3), 767–779.

Hoyer, M.V., Jones, J.R., 1983. Factors affecting the relation between phosphorus and chlorophyll a in midwestern reservoirs. Canadian Journal of Fisheries and Aquatic Sciences 40 (2), 192–199.

Hu, H.J., Wei, Y.X., 2006. The freshwater algae of China: systematic, taxonomy and ecology. Sciences Press, Beijing.

Huang, J., Gao, J., Hörmann, G., 2012. Hydrodynamic-phytoplankton model for short-term forecasts of phytoplankton in Lake Taihu. China. Limnologica 42 (1), 7–18.

Huisman, J., Codd, G.A., Paerl, H.W., Ibelings, B.W., Verspagen, J.M., Visser, P.M., 2018. Cyanobacterial blooms. Nature Reviews Microbiology 16 (8), 471–483.

Huisman, J., Jonker, R.R., Zonneveld, C., Weissing, F.J., 1999. Competition for light between phytoplankton species: experimental tests of mechanistic theory. Ecology 80 (1), 211–222.

Huisman, J., Sharples, J., Stroom, J.M., Visser, P.M., Kardinaal, W.E.A., Verspagen, J.M., Sommeijer, B., 2004. Changes in turbulent mixing shift competition for light between phytoplankton species. Ecology 85 (11), 2960–2970.

Jakobsen, H.H., Blanda, E., Staehr, P.A., Højgård, J.K., Rayner, T.A., Pedersen, M.F., Jepsen, P.M., Hansen, B.W., 2015. Development of phytoplankton communities: implications of nutrient injections on phytoplankton composition, pH and ecosystem production. Journal of Experimental Marine Biology and Ecology 473, 81–89.

Jia, J., Gao, Y., Zhou, F., Shi, K., Johnes, P.J., Dungait, J.A., Lu, Y., 2020. Identifying the main drivers of change of phytoplankton community structure and gross primary productivity in a river-lake system. Journal of Hydrology 583, 124633.

Jiang, P., Liu, X., Zhang, J., Yuan, X., 2016. A framework based on hidden Markov model with adaptive weighting for microcystin forecasting and early-warning. Decision Support Systems 84, 89–103.

Jones, J.R., Knowlton, M.F., 2005. Suspended solids in Missouri reservoirs in relation to catchment features and internal processes. Water Research 39 (15), 3629–3635.

Jørgensen, S.E., Bendoricchio, G., 2001. Fundamentals of ecological modelling, Vol. 21. Elsevier.

Kara, E.L., Hanson, P., Hamilton, D., Hipsey, M.R., McMahon, K.D., Read, J.S., Bertilsson, S., 2012. Time-scale dependence in numerical simulations: assessment of physical, chemical, and biological predictions in a stratified lake at temporal scales of hours to months. Environmental Modelling & Software 35, 104–121.

Klausmeier, C.A., Litchman, E., Daufresne, T., Levin, S.A., 2004. Optimal nitrogen–to-phosphorus stoichiometry of phytoplankton. Nature 429 (6988), 171–174.

Li, H., Barber, M., Lu, J., Goel, R., 2020. Microbial community successions and their dynamic functions during harmful cyanobacterial blooms in a freshwater lake. Water Research 185, 116292.

Li, S.J., Song, K.S., Zhao, Y., Mu, G.Y., Shao, T.T., Ma, J.X., 2016. Absorption Characteristics of Particulates and CDOM in Waters of Chagan Lake and Xinlicheng Reservoir in Autumn. Environmental Science 37 (1), 112–122 in Chinese.

Li, Y., Liu, Y., Zhao, L., Hastings, A., Guo, H., 2015. Exploring change of internal nutrients cycling in a shallow lake: a dynamic nutrient driven phytoplankton model. Ecological Modelling 313, 137–148.

Lie, A.A., Wong, C.K., Lam, J.Y., Liu, J.H., Yung, Y.K., 2011. Changes in the nutrient ratios and phytoplankton community after declines in nutrient concentrations in a eutrophic semi-enclosed bay in Hong Kong. Marine Environmental Research doi:10.1016/j.marenvres.2011.01.001.

Liu, X., Lu, X., Chen, Y., 2011. The effects of temperature and nutrient ratios on Microcystis blooms in Lake Taihu, China: an 11-year investigation. Harmful Algae 10 (3), 337–343.

Liu, X., Qian, K., Chen, Y., Gao, J., 2016. A comparison of factors influencing the summer phytoplankton biomass in China's three largest freshwater lakes: Poyang, Dongting, and Taihu. Hydrobiologia, pp. 1–20.

Liu, X., Zhang, G., Sun, G., Wu, Y., Chen, Y., 2019. Assessment of Lake water quality and eutrophication risk in an agricultural irrigation area: A case study of the Chagan Lake in Northeast China. Water 11 (11), 2380.

Liu, X., Zhang, G., Xu, Y.J., Wu, Y., Liu, Y., Zhang, H., 2020a. Assessment of water quality of best water management practices in lake adjacent to the high-latitude agricultural areas. China. Environmental Science and Pollution Research 27 (3), 3338–3349.

Liu, X., Zhang, G., Zhang, J., Xu, Y.J., Wu, Y., Wu, Y., Ma, H., 2020b. Effects of irrigation discharge on salinity of a large freshwater lake: A case study in Lake Chagan. Northeast China. Water 12 (8), 2112.

Los, F.J., 2005. An algal biomass prediction model. In: Loucks, D.P., Van Beek, E. (Eds.), Water resources systems planning and management—an introduction to methods, models and applications. UNESCO, pp. 408–416.

Los, F.J., 2009. Eco-hydrodynamic modelling of primary production in coastal waters and lakes using BLOOM, Vol. 1. Ios Press.

Los, F.J., Brinkman, J.J., 1988. Phytoplankton modelling by means of optimization: A 10-year experience with BLOOM II: With 4 figures in the text. Internationale

Vereinigung für theoretische und angewandte Limnologie. Verhandlungen 23 (2), 790–795.

Los, F.J., Villars, M.T., Van der Tol, M.W.M., 2008. A 3-dimensional primary production model (BLOOM/GEM) and its applications to the (southern) North Sea (coupled physical–chemical–ecological model). Journal of Marine Systems 74 (1-2), 259–294.

Los, F.J., Wijsman, J.W.M., 2007. Application of a validated primary production model (BLOOM) as a screening tool for marine, coastal and transitional waters. Journal of Marine Systems 64 (1-4), 201–215.

Lürling, M., Faassen, E.J., 2012. Controlling toxic cyanobacteria: effects of dredging and phosphorus-binding clay on cyanobacteria and microcystins. Water Research 46 (5), 1447–1459.

Markensten, H., Pierson, D.C., 2007. Weather driven influences on phytoplankton succession in a shallow lake during contrasting years: application of PROTBAS. Ecological Modelling 207 (2-4), 128–136.

McCarthy, J.J., Goldman, J.C., 1979. Nitrogenous nutrition of marine phytoplankton in nutrient-depleted waters. Science 203 (4381), 670–672.

Moriasi, D.N., Arnold, J.G., Van Liew, M.W., Bingner, R.L., Harmel, R.D., Veith, T.L., 2007. Model evaluation guidelines for systematic quantification of accuracy in watershed simulations. Transactions of the ASABE 50 (3), 885–900.

Moriasi, D.N., Gitau, M.W., Pai, N., Daggupati, P., 2015. Hydrologic and water quality models: Performance measures and evaluation criteria. Transactions of the ASABE 58 (6), 1763–1785.

Newcombe, G., Chorus, I., Falconer, I., Lin, T.F., 2012. Cyanobacteria: Impacts of climate change on occurrence, toxicity and water quality management. Water Research (Oxford) 46 (5), 240.

Oliver, R.L., Hamilton, D.P., Brookes, J.D., Ganf, G.G., 2012. Physiology, blooms and prediction of planktonic cyanobacteria. In: Ecology of cyanobacteria II. Springer, Dordrecht, pp. 155–194.

Paerl, H.W., Fulton, R.S., Moisander, P.H., Dyble, J., 2001. Harmful freshwater algal blooms, with an emphasis on cyanobacterial. The Scientific World Journal 1, 76–113.

Paerl, H.W., Havens, K.E., Xu, H., Zhu, G., McCarthy, M.J., Newell, S.E., Qin, B., 2019. Mitigating eutrophication and toxic cyanobacterial blooms in large lakes: The evolution of a dual nutrient (N and P) reduction paradigm. Hydrobiologia 847 (21), 4359–4375.

Paerl, H.W., Huisman, J., 2008. Blooms like it hot. Science 320 (5872), 57–58.

Paerl, H.W., Xu, H., McCarthy, M.J., Zhu, G., Qin, B., Li, Y., Gardner, W.S., 2011. Controlling harmful cyanobacterial blooms in a hyper-eutrophic lake (Lake Taihu, China): the need for a dual nutrient (N & P) management strategy. Water Research 45 (5), 1973–1983.

Preece, E.P., Hardy, F.J., Moore, B.C., Bryan, M., 2017. A review of microcystin detections in estuarine and marine waters: environmental implications and human health risk. Harmful Algae 61, 31–45.

Redfield, A.C., 1958. The biological control of chemical factors in the environment. American Scientist 46 (3), 230A–2221.

Reeder, B.C., 2017. Primary productivity limitations in relatively low alkalinity, high phosphorus, oligotrophic Kentucky reservoirs. Ecological Engineering 108, 477–481.

Reichwaldt, E.S., Ghadouani, A., 2012. Effects of rainfall patterns on toxic cyanobacterial blooms in a changing climate: between simplistic scenarios and complex dynamics. Water Research 46 (5), 1372–1393.

Ross, C., Santiago-Vázquez, L., Paul, V., 2006. Toxin release in response to oxidative stress and programmed cell death in the cyanobacterium Microcystis aeruginosa. Aquatic Toxicology 78 (1), 66–73.

Rousso, B.Z., Bertone, E., Stewart, R., Hamilton, D.P., 2020. A systematic literature review of forecasting and predictive models for cyanobacteria blooms in freshwater lakes. Water Research 115959.

Sakamoto, S., Lim, W.A., Lu, D., Dai, X., Orlova, T., Iwataki, M., 2020. Harmful algal blooms and associated fisheries damage in East Asia: current status and trends in China, Japan, Korea and Russia. Harmful Algae, 101787.

Schindler, D.W., 1977. Evolution of phosphorus limitation in lakes. Science 195 (4275), 260–262.

Schindler, D.W., Carpenter, S.R., Chapra, S.C., Hecky, R.E., Orihel, D.M., 2016. Reducing phosphorus to curb lake eutrophication is a success. Environmental Science & Technology 50, 8923–8929.

Scott, J.T., McCarthy, M.J., Paerl, H.W., 2019. Nitrogen transformations differentially affect nutrient-limited primary production in lakes of varying trophic state. Limnology and Oceanography Letters 4 (4), 96–104.

Smayda, T.J., 2008. Complexity in the eutrophication–harmful algal bloom relationship, with comment on the importance of grazing. Harmful Algae 8 (1), 140–151.

Smith, D.R., Haggard, B.E., Warnemuende, E.A., Huang, C., 2005. Sediment phosphorus dynamics for three tile fed drainage ditches in Northeast Indiana. Agricultural Water Management 71 (1), 19–32.

Smith, V.H., 1983. Low nitrogen to phosphorus ratios favor dominance by blue–Green algae algae in lake phytoplankton. Science 221, 669–671.

Smith, V.H., 1986. Light and nutrient effects on the relative biomass of blue-Green algae in lake phytoplankton. Canadian Journal of Fisheries and Aquatic Sciences 43 (1), 148–153.

Smith, V.H., Schindler, D.W., 2009. Eutrophication science: where do we go from here? Trends in Ecology & Evolution 24 (4), 201–207.

Smith, V.H., Tilman, G.D., Nekola, J.C., 1999. Eutrophication: impacts of excess nutrient inputs on freshwater, marine, and terrestrial ecosystems. Environmental Pollution 100 (1-3), 179–196.

Solovchenko, A.E., Khozin-Goldberg, I., Didi-Cohen, S., Cohen, Z., Merzlyak, M.N., 2008. Effects of light intensity and nitrogen starvation on growth, total fatty acids and arachidonic acid in the green microalga Parietochloris incisa. Journal of Applied Phycology 20 (3), 245–251.

Søndergaard, M., Lauridsen, T.L., Johansson, L.S., Jeppesen, E., 2017. Nitrogen or phosphorus limitation in lakes and its impact on phytoplankton biomass and submerged macrophyte cover. Hydrobiologia 795 (1), 35–48.

Sorokin, C., Krauss, R.W., 1958. The Effects of Light Intensity on the Growth Rates of Green Algae. Plant Physiology 33 (2), 109.

Stockwell, J.D., Doubek, J.P., Adrian, R., Anneville, O., Carey, C.C., Carvalho, L., belings, B.W., 2020. Storm impacts on phytoplankton community dynamics in lakes. Global Change Biology 26 (5), 2756–2784.

Su, X., Steinman, A.D., Tang, X., Xue, Q., Zhao, Y., Xie, L., 2017. Response of bacterial communities to cyanobacterial harmful algal blooms in Lake Taihu. China. Harmful Algae 68, 168–177.

Sun, S., Zhang, G.X., Huang, Z.G., Xu, C., L, R.R., 2014. Hydrological regimes of Chagan Lake in western Jilin Province. Wetland Science 12 (01), 43–48 (in Chinese).

Sun, J., Liu, D.Y., 1999. Study on phytoplankton biomass: Phytoplankton measurement biomass from cell volume or plasma volume. Acta Oceanologica Sinica 21 (2), 75–85.

Sunda, W.G., Huntsman, S.A., 1997. Interrelated influence of iron, light and cell size on marine phytoplankton growth. Nature 390 (6658), 389–392.

Teubner, K., Dokulil, M.T., 2002. Ecological stoichiometry of TN:TP:SRSi in freshwaters: nutrient ratios and seasonal shifts in phytoplankton assemblages. Archiv fur Hydrobiologie 154 (4), 625–646.

Torres-Águila, N.P., Martí-Solans, J., Ferrández-Roldán, A., Almazán, A., Roncalli, V., D'Aniello, S., Cañestro, C., 2018. Diatoms bloom-derived biotoxins cause aberrant development and gene expression in the appendicularian chordate Oikopleura dioica. Communications Biology 1 (1), 1–11.

Utkilen, H., Gjølme, N., 1995. Iron-stimulated toxin production in Microcystis aeruginosa. Applied and Environmental Microbiology 61 (2), 797–800.

Vrede, T., Ballantyne, A., MILLE-LINDBLOM, C., Algesten, G., Gudasz, C., Lindahl, S., Brunberg, A.K., 2009. Effects of N:P loading ratios on phytoplankton community composition, primary production and N fixation in a eutrophic lake. Freshwater Biology 54 (2), 331–344.

Wang, J., Zhang, Z., 2020. Phytoplankton, dissolved oxygen and nutrient patterns along a eutrophic river-estuary continuum: Observation and modeling. Journal of Environmental Management 261, 110233.

Wang, X., Zhang, J., Babovic, V., Gin, K.Y.H., 2019. A comprehensive integrated catchment-scale monitoring and modelling approach for facilitating management of water quality. Environmental Modelling & Software 120, 104489.

Wollheim, W.M., Peterson, B.J., Deegan, L.A., Hobbie, J.E., Hooker, B., Bowden, W.B., Finlay, J., 2001. Influence of stream size on ammonium and suspended particulate nitrogen processing. Limnology and Oceanography 46 (1), 1–13.

Xu, C., Zhang, J., Bi, X., Xu, Z., He, Y., Gin, K.Y.H., 2017. Developing an integrated 3D-hydrodynamic and emerging contaminant model for assessing water quality in a Yangtze Estuary Reservoir. Chemosphere 188, 218–230.

Yang, Y.N., Sheng, Q., Zhang, L., Kang, H.Q., Liu, Y., 2015. Desalination of saline farmland drainage water through wetland plants. Agricultural Water Management 156, 19–29.

Zeng, Q.H., Liu, Y., Zhao, H.T., Sun, M.D., Li, X.Y., 2015. Comparison of models for predicting the changes in phytoplankton community composition in the receiving water system of an inter-basin water transfer project. Environmental Pollution 223, 676–684.

Zhang, J., Jørgensen, S.E., Beklioglu, M., Ince, O., 2003a. Hysteresis in vegetation shift - Lake Mogan prognoses. Ecological Modelling 164, 227–238.

Zhang, J., Jørgensen, S.E., Tan, C.O., Beklioglu, M., 2003b. A structurally dynamic modelling—Lake Mogan, Turkey as a case study. Ecological Modelling 164 (2-3), 103–120.

Zhang, L., Hipsey, M.R., Zhang, G.X., Busch, B., Li, H.Y., 2017. Simulation of multiple water source ecological replenishment for Chagan Lake based on coupled hydrodynamic and water quality models. Water Science and Technology: Water Supply 17 (6), 1774–1784.

Zhang, W., Watson, S.B., Rao, Y.R., Kling, H.J., 2013. A linked hydrodynamic, water quality and algal biomass model for a large, multi-basin lake: a working management tool. Ecological Modelling 269, 37–50.

Zhu, Y.P., Zhang, H.P., Chen, L., Zhao, J.F., 2008. Influence of the South–North Water Diversion Project and the mitigation projects on the water quality of Han River. Science of the Total Environment 406 (1-2), 57–68.

Ziegmann, M., Abert, M., Müller, M., Frimmel, F.H., 2010. Use of fluorescence fingerprints for the estimation of bloom formation and toxin production of Microcystis aeruginosa. Water Research 44 (1), 195–204.

Zou, W., Zhu, G., Cai, Y., Vilmi, A., Xu, H., Zhu, M., Qin, B., 2020. Relationships between nutrient, chlorophyll a and Secchi depth in lakes of the Chinese Eastern Plains ecoregion: Implications for eutrophication management. Journal of Environmental Management 260, 109923.